Building and Environment 161 (2019) 106274

Contents lists available at ScienceDirect

Building and Environment

journal homepage: www.elsevier.com/locate/buildenv

Study on the acoustic characteristics of natural date palm fibres: Experimental and theoretical approaches

Ebrahim Taban[a], Ali Khavanin[a,*], Abdolreza Ohadi[b], Azma Putra[c], Ahmad Jonidi Jafari[d], Mohammad Faridan[e], Ardalan Soleimanian[a]

[a] Department of Occupational Health Engineering, Faculty of Medical Sciences, Tarbiat Modares University, Tehran, Iran
[b] Acoustics Research Lab, Mechanical Engineering Department, Amirkabir University of Technology, Tehran, Iran
[c] Centre for Advanced Research on Energy, Universiti Teknikal Malaysia Melaka, Hang Tuah Jaya, 76100, Durian Tunggal, Melaka, Malaysia
[d] Department of Environmental Health Engineering, School of Public Health, Iran University of Medical Sciences, Tehran, Iran
[e] Department of Occupational Health Engineering, School of Health and Nutrition, Lorestan University of Medical Sciences, Khorramabad, Iran

ARTICLE INFO

Keywords:
Natural fibres
Sound absorber
Date palm empty fruit
Sound absorption coefficient
Experimental and theoretical comparison

ABSTRACT

The present study deals with the acoustic performance of natural fibres originated from the date palm empty fruit (DPEFB) fibres which is mainly considered as agricultural waste. The fibres were processed and fabricated to be sound absorber samples with two different densities of 100 kg/m^3 and 200 kg/m^3 and with thicknesses of 10–40 mm. The normal incidence absorption coefficients of the sound absorbers were measured using an impedance tube based on ISO 10534-2. The effects of fibre density and sample thickness are discussed. The findings reveal that for density of 100 kg/m^3 the absorption coefficient is 0.6–0.8 above 1.5 kHz for the samples with the thickness of 20 mm and 30 mm. For the thickness of 40 mm, the values even reached the value of 0.9. The values can reach 0.7–0.8 above 1 kHz for the density of 200 kg/m^3. Mathematical model using the optimized Delaney-Bazley model with Nelder-Mead simplex method is shown to successfully predict the sound absorption coefficient of the fibre samples. The Johnson-Champoux-Allard model follows the trend of the absorption coefficient, but underestimates the measured data at high frequencies above 2.5 kHz.

1. Introduction

1.1. The main properties of natural fibres

Currently, engineering noise control measures such as the use of noise-absorbing materials are widely used to reduce the exposure levels of at-risk populations. Glass fibres, mineral wool, open cell foams and acoustic tiles, are among the mineral and synthetic fibrous or porous commercial absorbers that are usually employed to dissipate the sound energy in their interstices by visco-thermal phenomena. These synthetic absorbers have shown to be highly strong and durable, less thermal conductive and relatively fire retardant as well as resistant to the moisture absorption and the growth of bacteria and fungi [1]. Despite all these benefits, the application of such absorbers and insulators comes at a price. The production and use of these synthetic materials not only have negative impacts on the environment, mainly by contributing to global warming, but also poses significant risks to human health and well-being [2].

In order to tackle such shortcomings, a large number of studies have recently been progressing around the theme of using natural, biodegradable, recyclable and sustainable alternatives for the synthetically made acoustic absorbers. Table 1 summarises several recent studies conducted on the levels of acoustic absorption of some natural fibre materials.

Compared to the synthetic fibres, the use of their natural alternatives, either stand-alone or as a component of composite materials will offer considerable advantages, particularly in terms of environmental issues. Natural fibres are relatively cheap, available, abundant and usually have low densities. They are also a renewable resource, less abrasive to machines, equipment or tools and involved in enhanced CO_2 sequestration, lower emission of toxic fumes and gases during manufacturing or incineration as well as minimised dermal and respiratory irritation [21,22]. Such properties have therefore made these materials an innovative source for developing thermal and acoustical insulating materials, particularly in building sector of developing countries where the lack of proper recycling policies is a great concern [23].

Natural fibres are totally derived from animal, mineral or plant sources; of which the fibres with plant origin mainly consist of cellulose

* Corresponding author.
E-mail address: Khavanin@modares.ac.ir (A. Khavanin).

https://doi.org/10.1016/j.buildenv.2019.106274
Received 18 April 2019; Received in revised form 6 July 2019; Accepted 9 July 2019
Available online 10 July 2019

Table 1
A summary of recent studies investigating the acoustic absorption properties of several natural fibre materials.

Year	Fibres	Key findings	References
2019	Olive	The fabricated samples showed high levels of sound absorption coefficients particularly at higher frequencies as well as good agreement with predicting phenomenological models.	Martellotta [3]
2019	Coir	Thicker samples with constant densities showed increased levels of the sound absorption, especially at lower frequencies (< 1000 Hz).	Taban [4]
2018	Corn Husk	Natural corn husk fibre is capable of absorbing the sound energy and is appropriate for noise control purposes.	Xiong Yan [5]
2018	Pineapple	Average acoustic absorption coefficient for PALF is 0.9 above 2 kHz for thickness 20 mm and 0.8 above 1 kHz for thickness 30 mm for the constant fibre density	Putra [6]
2018	Kenaf	For the samples with the bulk density of 140–150 kg/m^3 and thickness of 25–30 mm, the absorption coefficient is above 0.5 starting from 500 Hz and can reach 0.85 on average above 1.5 kHz.	Putra [7]
2017	Oil palm	Sound absorption performance can be improved by increasing the thickness of the sample and also by having optimum densities of fibres.	Khai Hee Or [8]
2017	Broom	As generally expected for this type of materials, increase in the sample thickness brought about superior sound absorption at lower frequencies.	Berardi [9]
2016	Sugarcane	Decreasing the fibre size leads to the increase in the flow resistivity and the acoustic absorption coefficient.	Mohamed Taktak [10]
2016	Flax	The flax fibre reinforced composites come up with 25% higher sound absorption coefficient when compared to the glass fibre reinforced composites at lower frequency range.	Prabhakaran [11]
2015	Kapok	Increasing the level of greater porosity and creating pores with smaller diameters improves the sound absorption at lower frequencies.	Xiong Yan [12]
2015	Kenaf/Hemp/ coconut	Employing the natural fibres for sound absorption applications in buildings is beneficial.	Berardi [13]
2015	Luffa	Samples fabricated from luffa fibres yield higher sound absorption coefficients even for sample with smaller thickness (i.e. t = 12 mm).	Koruk [14]
2014	Banana	The maximum noise reduction coefficient is observed in the bulk density of 154 kg/m^3 at frequency ranges 250 Hz–4000 Hz with average value of 0.55.	Tholkappiyan [15]
2012	Hemp	Alkalization of the fibres under higher temperatures increases the flow resistivity and sound absorption performance.	Yilmaz [16]
2011	Jute	Compared to the glass fibres jute fibres show fair levels of acoustical attenuations and fire-retardant properties.	Fatima [17]
2011	Coir	Average absorption of 0.8 for f > 1360 Hz, f > 940 Hz, and f > 578 Hz observed for samples with thicknesses of 20 mm, 30 mm and 40 mm, respectively.	Fouladi [18]
2009	Tea-leaf fibre	The experimental data indicated that a 1 cm thick tea-leaf-fibre waste material with backing provides sound absorption which is almost equivalent to that provided by six layers of woven textile cloth.	Haluk Kücük [19]
2002	Bamboo	The values of sound absorption coefficients increased in the mid and high-frequency range when the density increased.	Koizumi [20]

fibrils embedded in lignin matrix and usually based on what part of the plants they are created from, these lignocellulosic natural fibres are divided into general categories of bast fibres, leaf fibres, seed hair fibres and fruit [24].

Despite all the advantages of the natural fibres, certain drawbacks such as poor water and fire resistance, weak fibre matrix bonding, and lower durability are associated with the use of them particularly in industrial settings. Therefore, different strategies including the physical, mechanical and chemical pre/treatments of the raw fibres have been proposed to modify or enhance their structural and surface properties; sometimes as composite materials.

Additionally, various types of binders and adhesives (usually made of bio-degradable materials) such as latex, poly vinyl alcohol (PVA), corn starch, glue, white cement, etc. have also been used to principally improve the levels of bonding between the natural fibres in the prepared samples.

For instance, biodegradable binders such as PVA have shown fair interaction with the natural fibres, resulting in satisfactory composite properties and acceptable performance. The PVA/natural fibres reinforced composites have also demonstrated good fibre/matrix bonding along with high tensile strength and Young's modulus [25]. Chen et al. [26] showed that coating the windmill palm fibres with PVA will significantly improve their sound absorption capability.

Othmani et al. [10] showed that the decrease in the binder content (resin) of the samples made from sugarcane wastes based materials resulted in an increase in the level of flow resistivity and thus an increase in the values of acoustic absorption coefficient. They concluded that minimizing the proportion of the binder in the composite would create more porosity and higher sound absorption coefficients.

The results from the study conducted by Wong et al. [27] indicated that the introduction of natural rubber latex as the binder to the samples made of spent tea leaves would relatively improve their acoustic properties. Although the addition of latex binder had blocked most of the pores of the samples with the finest fibres hence suppressing the absorption performance, the samples made of coarser fibres demonstrated better sound absorption coefficients mainly because of being more porous and dissipating sound waves by friction. They also reported that the samples fabricated with the finest fibres had the most significant absorption performance in terms of frequency with the maximum sound absorption coefficient shifting to relatively lower frequency range.

In reviewing the literature, determination of the acoustic absorption coefficients of natural fibres have been routinely conducted by methods such as the direct measurement with an impedance tube or numerical study using the empirical models of sound propagation in these materials [13].

Dunne et al. [27] in a review article investigated the factors that influence the sound absorption and the available empirical models for the prediction of the sound absorption coefficients of natural porous fibrous materials. Although the authors concluded that the available empirical models are not perfectly adequate for the prediction of sound absorption coefficient for several types of natural fibres, it is evident that these models are able to provide the designers with a general insight into the acoustic properties of such materials particularly in terms of reducing the costs and saving time during the design phase.

For instance, referring to the limits of Delany–Bazley model, Berardi et al. [29] employed a best-fit approach to fit their experimental results (normal incidence sound absorption coefficients of several natural materials) to the formulas of this model in order to inversely determine the eight numerical coefficients using an optimization process by the Nelder-Mead simplex method.

The study performed by Othmani et al. [28] which employed the Delany-Bazley, Lafarge-Allard and Johnson-Allard models to estimate the absorption coefficient of the samples fabricated from sugarcane wastes also revealed significant sound absorbing coefficients for these samples as well as good agreement between the measured values by the impedance tube and the ones predicted by Johnson-Allard the model.

The objective of this paper is to study the acoustic absorption coefficient of the natural fibres extracted from the date palm empty fruit bunches (DPEFBs). To the best of our knowledge, although several studies have already investigated the acoustic properties of the samples made from date palm fibres [29–32], no research in particular has yet considered the sound absorption characteristics (experimentally or theoretically) of natural fibres originated from DPEFBs.

In the first section of the paper, the sample preparation process and physical characteristics of each sample is detailed. In the second section, the experimental setups for the measurement of the absorption coefficient are presented. Mathematical sound absorbing models aiming to predict the absorption properties of these samples are also presented in this paper. In the last part of this paper, the effects of physical parameters on sound absorption are reported and the theoretical and experimental results are compared.

1.2. Date palm fibres

Iran has always been the home to vast plantations of date palm (Phoenix dactylifera L.) since ancient times and over the course of history. In fact, Iran is the second largest producer of fresh date in the world by producing more than 1000,000 metric tons annually [33]. According to the Iranian Ministry of Agriculture, there are more than 400 species of dates all over the country, but only a few of them are commercially available. It is estimated that the waste from pruning each palm tree in Iran is about 17–34 kg. Therefore, by considering the fact that more than 20 to 27 million palm trees exist in Iran, around 200,000 tons of wastes from the date palms in the form of fibrous lignocellulosic materials are produced annually. Table 2 shows the average proportion of the contents of each date palm wastes. Although there have been attempts to utilize date palm tree by-products, since there are no proper alternative applications for such staggering amount of wastes and due to poor agricultural waste management, they are usually considered as a nuisance by many Iranian farmers and large quantities of them are either burned or buried within the plantations [34,35].

2. Materials and methodology

2.1. Preparation of samples

The date palm natural fibre originated from the empty fruit bunches of the palm trees were obtained from a date palm plantation located in the city of Tabas, South Khorasan province, Iran. The DPEFB fibres were first cut into small pieces using a manual shredder and then dried in an autoclave at 70 °C for 24 h. The fibres were then sieved through a 2.0 mm mesh size sieve and were stored in desiccators to decrease their moisture content to less than 10% before the sound absorption test was performed. In order to meet the set densities of 100 and 200 kg/m^3, the DPEFB fibres mass was measured accurately.

The DPEFB fibres were then soaked with polyvinyl alcohol (PVA) in order to bind them to one another. PVA is a widely used suitable binder owing to characteristics such as biodegradability, high polarity, good mechanical properties and easy processability [25]. In order to prepare the PVA solution, 5 g of PVA powder (99.000 g/mol - Sigma-Aldrich) was dissolved in 100 ml of distilled water in a beaker placed on a magnetic stirrer (500 rpm) at 80 °C for 3 h per the body. The prepared solution was then applied to the DPEFB fibres and the fibre mixture was fitted into two cylindrical stainless-steel moulds with internal diameters of 30 and 100 mm prior to compression process in a manual hydraulic press machine (200 bars, 30 min). Each mould consisted of two half-cylinders with a bottom plate to the one side. While two rings were used for fixing the two halves of the mould, the fibres were pressed inside by applying pressure on top surface of them with a punch. Use of several inner spacer plates facilitated the formation of the samples with different thicknesses within the mould. The prepared cylindrically-shaped samples were eventually transferred to an anechoic chamber for conducting the acoustic absorption coefficient measurement using an impedance tube. Fig. 1 illustrates the steps from the sample preparation process along with the experimental testing.

Table 2
Proportion of the contents of date palm wastes.

Contents	Amount (Kg)	Proportion of each content to the total amount of wastes (%)
Leaves (Leaflets, Rachis, Spines)	18	52.94
Empty fruit bunches	6	17.65
Petioles	7	20.59
Trunk fibres	3	8.82
Total	34	100

2.2. Measurement of physical properties

2.2.1. Porosity

Porosity is one of the most important physical parameters influencing the acoustic absorption of the materials. It is usually defined as the ratio of pore volume to the total volume of a porous material.

The porosity of the samples fabricated from DPEFB fibres in this study was determined indirectly from the fibre density data, ρ_{fibre} and the bulk density, ρ_{bulk} given by

$$\rho_{bulk} = (1 - \varphi)\rho_{fibre} \quad (1)$$

where ρ_{bulk} can be calculated from the ratio of mass of the sample to its total volume (including the volume of the pores).

Measurements based on the Scanning Electron Microscope (SEM) revealed that the outer diameter of the DPEFB fibres was within the range of 200–720 μm and the thickness of the cell wall was less than 5 μm (see Fig. 2). The average diameter and the average density of the fibres together with the binder mixture are 465 μm and 930 kg/m^3, respectively. This measured fibre density and the bulk density for each sample provide the values of porosity (φ) to be more than 80%. As observed in Fig. 2, the hollow structure in the DPEFB fibres also contributes to the porosity of the sample.

2.2.2. Static airflow resistivity

Flow resistivity is defined as the pressure drop of a fluid flow with a given velocity when it passes through a material. The air flow resistivity of the sample is calculated as

$$\sigma = A(p_2 - p_1)/Qd \quad (2)$$

where d is the sample thickness, A is the cross-sectional area and p_1 and p_2 are the values of pressure at front and back surfaces of the sample when the air passes across with volumetric flow rate Q.

The air flow resistivity of the samples was measured according to the ISO 9053 standard [36]. For each sample, the measurement process was repeated three times and the average value was recorded.

2.2.3. Tortuosity

Tortuosity, α_∞ is a dimensionless parameter which delineates the spatial orientation of adjacent internal pore structures in a porous material in relation with the macroscopic velocity of the fluid flow through the material [37]. Tortuosity represents the complexity of acoustic path in a porous material. The more complex the path, the greater the sound energy loss in the material.

2.2.4. Viscous and thermal characteristic lengths

The viscous characteristic length, Λ is the parameter firstly introduced by Johnson et al. [38] to be used to predict the frequency dependent, dynamic tortuosity and the dynamic density in the pores, especially for a porous medium with a network of non-intersecting

Fig. 1. DPEFB Sample preparation and acoustic absorption testing.

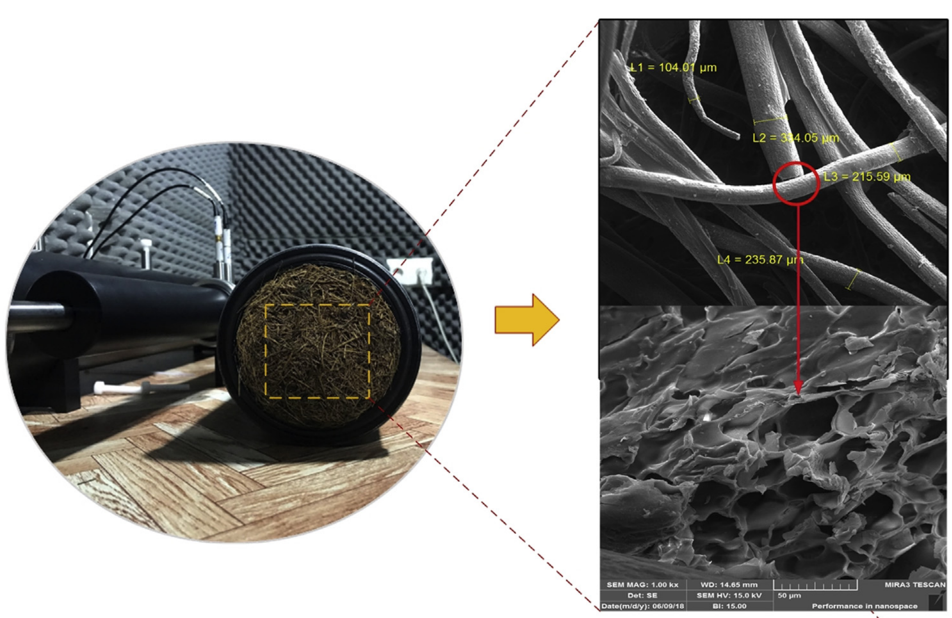

Fig. 2. The cross section of sample made from DPEFB fibres under SEM.

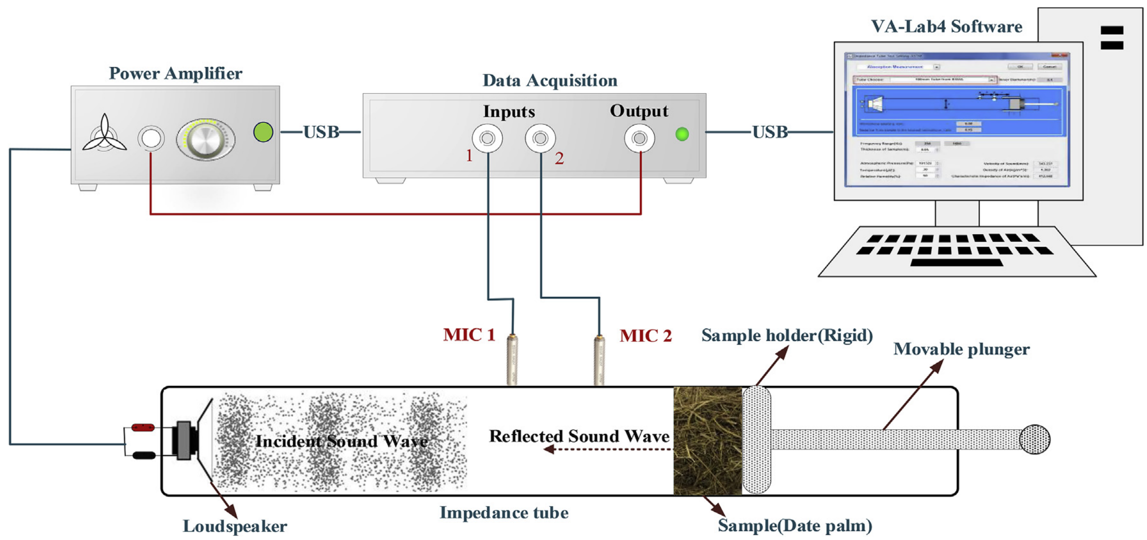

Fig. 3. Schematic diagram of the acoustical measurement system (BSWA, China).

tubes with a uniform cross-section. For materials with non-uniform pores, another parameter which is the thermal characteristic length, Λ' needs to be accounted and this was proposed by Champoux and Allard [39] through dynamic bulk modulus. The combination of the dynamic tortuosity, dynamic density and dynamic bulk modulus is usually called the Johnson-Champoux-Allard model.

While it is difficult to physically interpret the viscous characteristic length, the thermal characteristic length might be related the internal surface area of the pore. Nonetheless, Horosenkhov et al. [40] proposed asymptotic models to relate these two parameters specifically, to the pore size distribution in the materials which can be conveniently measured non-acoustically, namely the media pore size and the standard deviation in the pore size.

2.3. Measurement of absorption coefficient

The measurement of normal incidence absorption coefficient was carried out according to ISO 10534-2 using an impedance tube. Fig. 3 shows the experimental set up for the measurement of the sound absorption coefficients. The impedance tube equipped with two microphones, a loudspeaker and a frequency analysis. Located at one end of the tube, a loudspeaker generated broadband random sound waves which were then transmitted to the surface of the sample fitted in a sample holder at the other end. The reflected signals were recorded by the microphones mounted at two fixed points on the tube wall prior to the calculation of normal incidence absorption coefficient by the analyser. BSWA VA-Lab4 Basic software was employed to perform the data processing. Before the measurement, the microphones were calibrated with BSWA calibrator at frequency of 1 kHz and 114 dB sound pressure level.

The impedance tube system used in the experiment consisted of a large diameter tube (100 mm) and a small diameter tube (30 mm) to measure the absorption coefficients at low frequencies (63–1600 Hz) and high frequencies (1600–6300 Hz), respectively. The full frequency range for the sound absorption coefficients presented in this report is the combination of the values measured in the two tubes which gives the measured frequency range of 63–6300 Hz.

The samples with different thicknesses and bulk densities were appropriately fitted into the holders of the smaller and larger tubes where the sample or the cavity behind the sample could be adjusted by a rigid plunger. The measurement of the sound absorption coefficient was performed at least three times for each sample. In order to minimize the risk of error due to the misalignment of the samples inside the sample holder, for each sequence of sampling, the sample was taken out from the tube and again reinstalled into the holder. All the tests were conducted at controlled atmospheric conditions of (20 ± 2) °C relative humidity of (45 ± 10) % and pressure of 1.01325 × 105 Pa.

2.4. Modelling of absorption coefficient

In order to predict the sound absorption coefficients of the samples made from DPEFB fibres three different models were employed in this study.

2.4.1. Delany-Bazley's model

The model presented by Delany and Bazley (D&B) in 1970 is the very first of its kind and provides a simple, fast and semi-empirical approach for calculating the surface characteristic impedance and the propagation constant as a function of the flow resistivity of porous materials [41]. It was developed by using power-law relations by curve fitting a large amount of measured data of fibrous materials. This model utilizes the following formulation for the approximation of acoustical characteristics:

$$Z_c = \rho_0 c_0 \left[1 + 0.0571(X)^{-0.754} - i0.087\left({}^{\rho_0 f}\!/_{\sigma} \right)^{-0.732} \right] \tag{3}$$

$$K_c = {}^{\omega}\!/_{c_0} \left[1 + 0.0978(X)^{-0.7} - i0.189\left({}^{\rho_0 f}\!/_{\sigma} \right)^{-0.595} \right] \tag{4}$$

$$X = {}^{\rho_0 f}\!/_{\sigma} \tag{5}$$

$$Z_s = -jZ_c \cot(kd) \tag{6}$$

$$R = \frac{Z_s - \rho_0 c_0}{Z_s + \rho_0 c_0} \tag{7}$$

where ρ_0 is the density of air; c_0 is the speed of sound in the air; Z_c is the characteristic impedance; K_c is the propagation constant; f is the frequency; ω is the angular frequency; σ is the static airflow resistivity; R is sound pressure reflection coefficient; Z_s is the surface impedance; d is the thickness of the sample.

The absorption coefficient is calculated by

$$\alpha = 1 - |R|^2 \tag{8}$$

Despite the benefits and simplicity of D&B model for predicting the sound absorption coefficient of several types of mineral and synthetic materials, it has been shown to be limited in terms of its range of validity as well as being unable to perfectly predict the acoustic

Table 3
Revised expressions of the Delany–Bazley power-law functions for DPEFB fibres in this paper.

Sample ID	Thickness	Density	C1	C2	C3	C4	C5	C6	C7	C8
Sample #1	10	100	0.3656	1.6636	−0.2736	0.8318	0.3007	0.3417	−0.0549	−1.6011
Sample #2		200	0.0004	3.0089	0.1141	1.3838	0.3903	0.9245	−0.0600	−0.1013
Sample #3	20	100	1.2062	3.1018	0.0004	−8.2030	0.5877	1.2099	0.0450	3.1514
Sample #4		200	−0.0183	−3.2380	0.3181	1.3523	0.1872	2.1282	−0.0923	3.2940
Sample #5	30	100	0.6925	1.1046	−0.0038	3.1181	0.2893	0.3427	0.1986	−1.9305
Sample #6		200	0.4333	1.1175	−0.4956	0.4389	0.4099	−1.1589	0.1161	1.3536
Sample #7	40	100	0.0914	1.7678	0.4359	1.4095	0.5856	0.9796	−0.0730	−2.1863
Sample #8		200	0.0003	2.210	0.0662	0.8461	0.1987	0.5472	0.6399	−0.6002

absorption of samples made of thicker natural fibers [13,42]. Moreover, the accurate measurement of airflow resistivity as the main parameter of this model seems to be fairly demanding for natural fibres due which is mainly to the presence of non-laminar air flow and dealing with very low pressure difference on the two sides of the sample.

Due to these shortcomings, several attempts by many authors have been made to either improve the validity of prediction or extend such validity to broader range of materials. For instance, Miki [43] and Komatsu [44] introduced several constraints to the D&B's model formulation to achieve more physically valid values for the propagation coefficient and characteristic impedance as well as improving D&B's original measured data at lower frequencies.

In this paper we followed the best-fit inverse methodology proposed by Berardi and colleagues [45] as the starting point to obtain the c_i (with $i = 1, 2, \dots 8$) coefficients by fitting the experimental results to D&B's formulas. Through an optimization process by Nelder-Mead simplex method, the c_i coefficients are obtained (Table 3). The squared difference between the measured sound absorption coefficient and the corresponding estimated absorption coefficient are then calculated using Eqs. (9) -(11) in order to determine the error function.

$$Z_c = \rho_0 c_0 \left[1 + c_1\left(\frac{\rho_0 f}{\sigma}\right)^{-c_2} - j \times c_3\left(\frac{\rho_0 f}{\sigma}\right)^{-c_4}\right] \tag{9}$$

$$K_c = {}^{\omega}/_{c_0}\left[c_5\left(\frac{\rho_0 f}{\sigma}\right)^{-c_6} + j \times \left(1 + c_7\left(\frac{\rho_0 f}{\sigma}\right)^{-c_8}\right)\right] \tag{10}$$

$$\frac{\partial \varepsilon}{\partial A_i} = 2\sum_{i=1}^{N}(\alpha_{n,i} - \hat{\alpha}_{n,i})\frac{\partial \hat{\alpha}_{n,i}}{\partial A_i} = 0 \quad i = 1, \dots, 8 \tag{11}$$

2.4.3. Johnson-Champoux-Allard's model

Johnson-Champoux-Allard's model (JCA) [46] is a phenomenological rigid frame model, which assumes that the fibres are more rigid and heavier than the fluid and thus the porous medium can be approached as an 'equivalent fluid' inside a rigid frame. This model takes into account five physical parameters in the calculation, namely the airflow resistivity σ, porosity φ, tortuosity α_∞, viscous characteristic length Λ, and thermal characteristic length Λ'. Accordingly, the following formulations of effective density, $\rho(\omega)$ and bulk modulus, $K(\omega)$ are used and are given by

$$\rho(\omega) = \alpha_\infty \rho_0\left[1 + \frac{\sigma\varphi}{j\omega\rho_0\alpha_\infty}\left(1 + \frac{4i\alpha_\infty^2\eta\omega\rho_0}{(\sigma\Lambda\varphi)^2}\right)^{1/2}\right] \tag{12}$$

$$K(\omega) = kp_0\left(k - \left(k-1\right)\left[1 + \frac{\sigma'\varphi}{i\omega\rho_0\alpha_\infty N_{pr}}\left(1 + \frac{4i\alpha_\infty^2\eta N_{pr}\omega\rho_0}{(\sigma'\Lambda\varphi)^2}\right)^{1/2}\right]^{-1}\right)^{-1} \tag{13}$$

with

$$\sigma' = \frac{8\eta\alpha_\infty}{\Lambda'^2\varphi} \tag{14}$$

$$Z_c(\omega) = \sqrt{\rho_{(\omega)} \cdot K_{(\omega)}} \tag{15}$$

$$K_c(\omega) = \omega\sqrt{\frac{\rho_{(\omega)}}{K_{(\omega)}}} \tag{16}$$

where N_{pr} is the Prandtl number for air, η is the air viscosity, k is the special heat for air. It can be seen that the air condition is important in the calculation of density and bulk modulus equivalent.

Finally, the surface acoustical impedance Z_s at normal incidence for a sample with thickness d is given as

$$Z_s = -i\frac{Z_c(\omega)}{\varphi}.\ \cot(K_c(\omega).\ d) \tag{17}$$

As the porosity and air flow resistivity of the samples were obtained from experiment, the other three physical properties, namely the tortuosity, α_∞, the viscous characteristic length, Λ and the thermal characteristic length, Λ′ were obtained using the inverse acoustical characterization approach [43]. We followed a technique based on the method proposed by Atalla and Panneton [47] and Olny and Panneton [48] which utilizes the measured absorption coefficient along with coding in the MATLAB software and differential evolution algorithm in order to calculate the three unknown properties until the difference between the measured and the simulated absorption coefficient is converging to a minimum value.

The values of the physical parameters which are required to determine the absorption coefficients of the eight samples of the DPEFB fibers through the mathematical modellings are summarized in Table 4. The flow resistivity and porosity were obtained from measurement, while the tortuosity and the characteristic lengths were calculated from JCA model fitted with the measured absorption coefficient. The latter is presented in Section 3.4.

3. Results and discussion

The measured data are discussed here based on the parametric study of the density of DPEFB fibres. The effect of thickness is also presented together with the comparison of results using the proposed existing mathematical models as in Section 2.4. The measured absorption coefficients of DPEFB fibers are also compared with those of several other natural fibers in order to provide more insight about the acoustic absorption of different samples.

3.1. Effect of density and thickness

The bulk density of a porous material (the total mass per its unit volume) has a great influence on the porosity and flow resistivity of the porous materials and therefore directly influences the sound absorption performance. In this study, the samples were fabricated with two bulk densities of 100 and 200 kg/m^3, each with various thicknesses.

Fig. 4 demonstrates the effect of density on the sound absorption of the samples fabricated from DPEFB fibers. Both densities show absorption coefficient greater than 0.5 above 1 kHz, except for samples with thickness of 10 mm.

Table 4
Basic Properties and physical parameters for the acoustic model.

Sample ID	Thickness (mm)	Bulk density (kg/m^3)	Measured Flow resistivity σ ($Nm^{-4}s$)	Porosity $\varnothing$(%)	Tortuosity α_∞	Characteristic lengths (μm)	
						Λ	Λ'
Sample #1	10	100	1940	89.23	2.33	153	311
Sample #2	10	200	5910	78.49	2.39	165	341
Sample #3	20	100	1785	89.76	2.8	189	414
Sample #4	20	200	5768	78.98	3.8	147	506
Sample #5	30	100	1673	90.23	1.91	149	566
Sample #6	30	200	5580	80.33	1.83	135	430
Sample #7	40	100	1535	90.58	1.18	112	413
Sample #8	40	200	5470	80.87	1.00	92	378

Average Diameter of fibre (μm): 465
Average Density of fibre(kg/m^3): 930

As already well-known, increasing the thickness of acoustic material (while maintaining the fibre density constant) improves the absorption coefficient both in terms of the amplitude and the frequency bandwidth. Improvement towards low frequency range can be seen as more sound energy with longer wavelength can be absorbed. The thicker the sample, the greater dissipation of sound traversing the sample by visco-thermal interactions contributes to the greater normal incidence absorption coefficient. For the thickness of 40 mm, the absorption coefficients significantly increase to 0.9 on average above 1.5 kHz, while for the thickness of 20 mm and 30 mm, the values are around 0.6–0.8.

For an acoustic panel with rigid back, the tortuosity can affect the resonance within the materials and thus determines the absorption performance. As presented in the study by Jiménez et al. [49], the layer thickness can be strongly reduced below the quarter-wavelength resonance. This effect becomes greater towards lower frequencies and increases as the tortuosity increases. Table 4 shows the tortuosity value obtained from the fitted JCA model where the tortuosity is almost similar for each thickness with different densities except for thickness of 20 mm, where the fitted tortuosity for the 200 kg/m^3 sample (3.8) is higher than that (2.8) for the 100 kg/m^3 sample. The peak absorption can be obviously seen to shift to a lower frequency for thickness of 20 mm in Fig. 4.

3.2. Effect of air gap

Introducing an air gap has been a well-established method in practical application, particularly for a thin acoustic panel to improve the absorption coefficient towards the lower frequencies [50]. For a panel where the thickness is much smaller than the air gap (thin sheet or membrane), the absorption is maximum at the resonance frequency equivalent to the quarter wavelength of the introduced air gap [51]. Similar treatment has been applied for a porous absorber with a finite thickness and is found to be practically useful without having to add more fibres to form a thicker absorber panel.

For the sake of brevity, we only present the effect of air gap on the sound absorption coefficient of the samples with the thickness of 30 mm and densities of 100 kg/m^3 and 200 kg/m^3 (as presented in Fig. 5). The air gaps introduced behind the samples were 10 mm, 20 mm and 30 mm. As expected, introducing an air gap behind the samples shifted the peak absorption coefficients towards the lower frequencies. Such increase however is accompanied with the reduction of acoustic absorption coefficients at higher frequencies mainly due to the formation of standing waves in the air gap behind the sample.

For the thicker samples of 20 mm, the peaks of absorption appearing at around 1–2 kHz are more obvious. These peaks however cannot be expected to be exactly at the frequencies of the quarter wavelength of the air gap, as the mechanism of absorption is different compared to the thin panel where the resonance is determined by the local movement of particle mass at the panel and the stiffness of the air layer behind the panel.

As mentioned earlier, introduction of airgap can be an efficient strategy to have thinner samples to behave more like thicker samples in terms of acoustic absorption. For instance, Fig. 6 demonstrates that the acoustic absorption levels provided by the sample with the thickness of

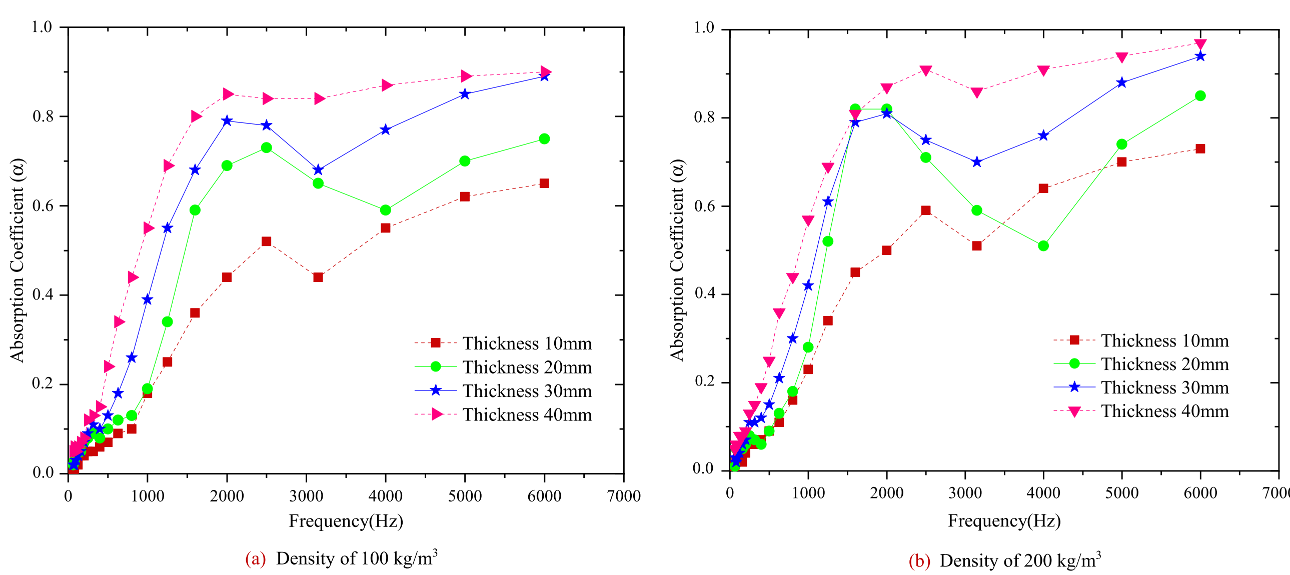

Fig. 4. Sound absorption coefficients of the samples of DPEFB fibres with different densities and thicknesses.

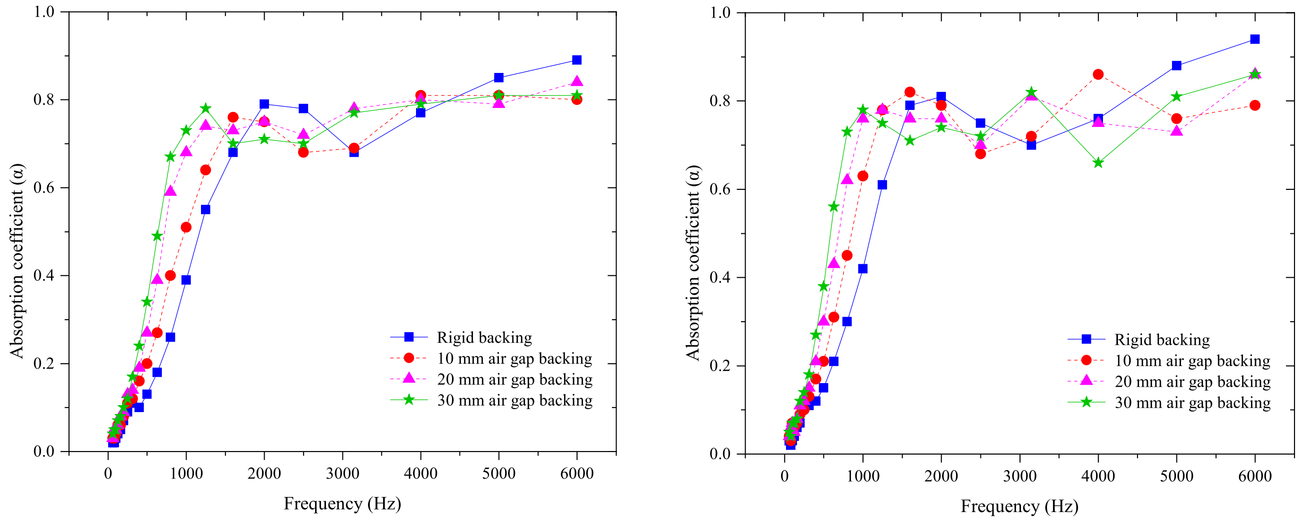

(**a**) Density of 100 kg/m^3 (**b**) Density of 200 kg/m^3

Fig. 5. Sound absorption coefficient of DPEFB fibres with thickness of 30 mm with different air gap backings.

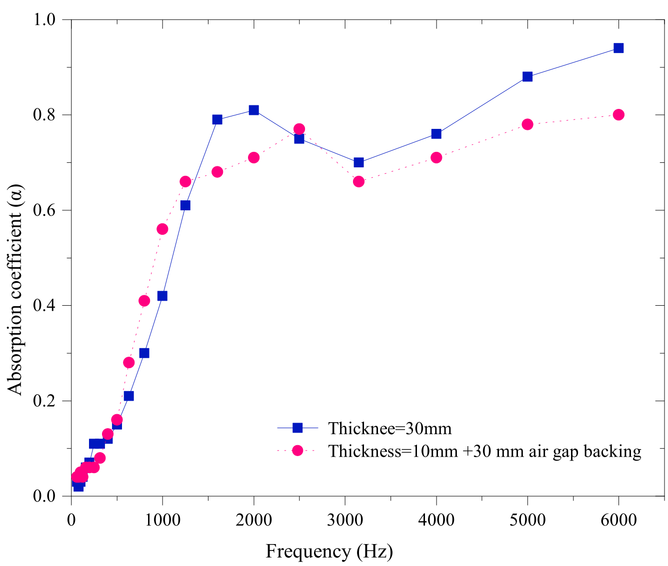

Fig. 6. The comparison of sound absorption coefficient between sample with thickness 30 mm with rigid backing and that with thickness of 10 mm and air gap of 30 mm.

30 mm and rigid backing is almost similar to the one with 10 mm thickness and air gap of 20 mm.

3.3. Comparison with several other natural fibers

Providing more insight about the results, the sound absorption coefficients of a sample fabricated from DPEFB fibers with a bulk density of 100 kg/m^3 and the thickness of 30 mm was compared to several samples made of identical natural fibers (with the same thickness) which were tested in the previous studies [4,8,28,52,53].

As can be seen in Fig. 7, although the results from the obtained absorption coefficients of DPEFB sample is almost comparable to the samples of coir and sugarcane particularly at frequencies below 2.5 kHz, other samples such as the oil palm, hemp and kenaf have generally come up with superior coefficients. In other words, this comparison restates the fact that multiple parameters such as bulk density and diameter of fibres are involved in shaping their acoustic absorption behavior. While the oil palm sample with a bulk density three times larger than our DPEFB samples showed greater absorption

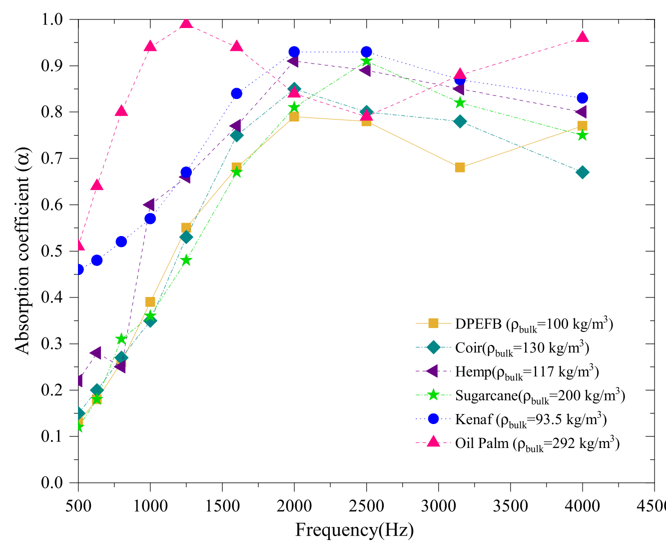

Fig. 7. Comparison of sound absorption coefficient of DPEFB with other natural fibres (thickness = 30 mm).

coefficients, kenaf and hemp samples with almost same bulk density with DPEFB fibres also demonstrated higher absorption coefficients.

3.4. Comparison with mathematical models

Figs. 8–11 present the absorption coefficients in terms of density and thickness and these measured data are compared with the mathematical models, namely D&B and JCA as explained in Section 2.4.

It should also be noted that the empirical formulae derived by Delaney and Bazley was based on the measured results from fiberglass and rockwool materials having short fibres smaller than 15 μm in diameter [41]. Given the limits of the D&B model for predicting the sound absorption coefficients of the natural fibers, we took the best-fit inverse approach proposed by Berardi and colleagues [45] in order to compare the results with the ones achieved by the experiments. The MATLAB coding along with the Nelder-Mead Simplex method was utilized to determine the optimized c_i coefficients of the D&B model formulas by minimizing the error between the measured values and predicted ones. Thereby, the acoustic impedance and the propagation constant were obtained for predicting the normal sound absorption coefficients of the

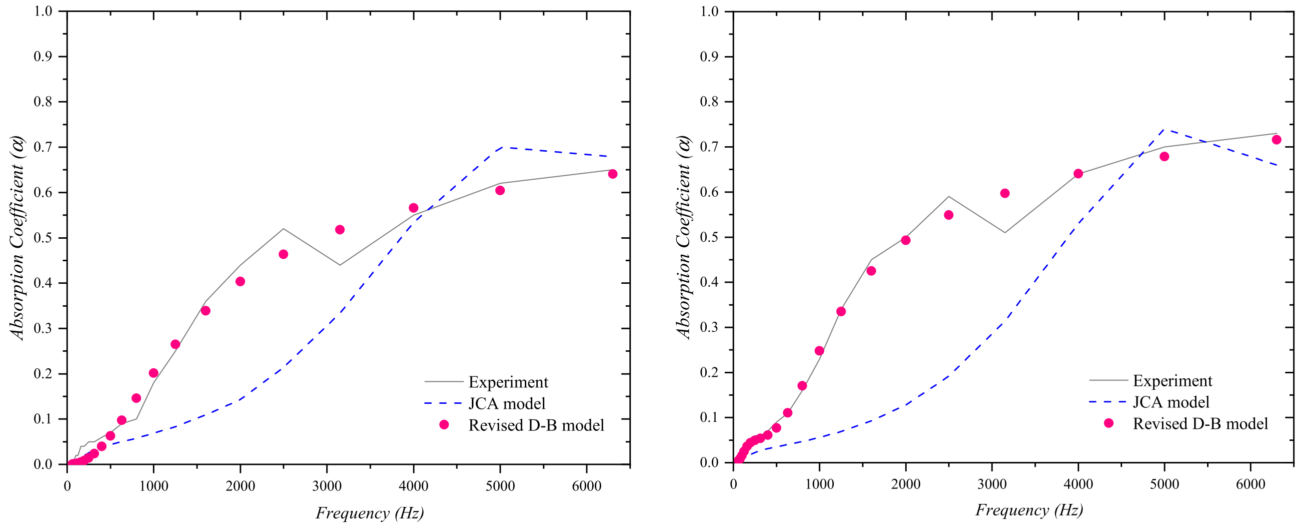

(a) Density of 100 kg/m^3

(b) Density of 200 kg/m^3

Fig. 8. Comparison of the sound absorption coefficients of DPEFB fibres samples (10 mm thickness) obtained from experiment vs. mathematical models.

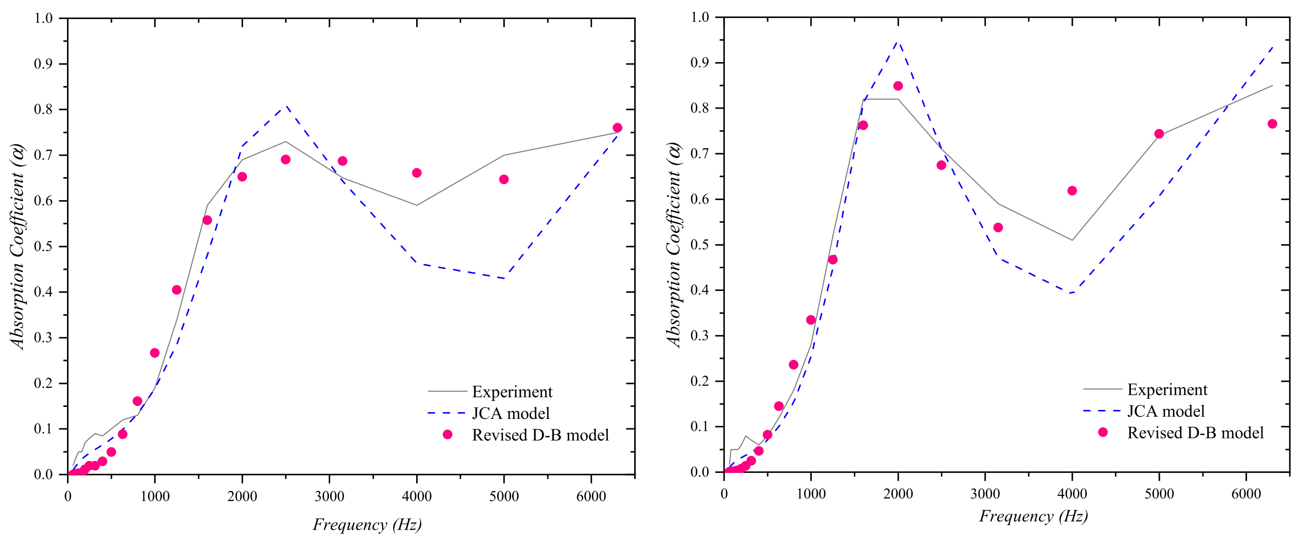

(b) Density of 100 kg/m^3

(b) Density of 200 kg/m^3

Fig. 9. Comparison of the sound absorption coefficients of DPEFB fibres samples (20 mm thickness) obtained from experiment vs. mathematical models.

DPEFB samples within the frequency range of 0–6 kHz.

As can be seen in Figs. 8–11, the revised D&B model gives good fits to the measured results, which is an indication that the derived coefficients c_i are sufficiently accurate to predict the acoustic absorption levels of the samples. Such inverse approach again demonstrates that the acoustic behavior of natural fibers can be modeled by simple models that require only finite set of variables. Moreover, high density and high flow resistivity of DPEFB samples resembles those of glassfibres and rockwool and these may have compensated the non-similarity of fibre size and hardness between these mineral materials and the natural DPEFB fibres which ends up with good approximation on D&B empirical prediction. The applied best-fit approach here however cannot be generalized to the other types of natural fibers mainly due to distinctive fiber diameters, bulk densities and samples airflow resistivity.

Apart from the 10 mm thick samples, which could be due to the uncertainty from the characterized input parameters, the values predicted by JCA model can be seen to have fair agreement with the experimental results. The inaccuracy for 10 mm thickness might be contributed by the uncertainty in the measurements of the porosity, air flow resistivity or the absorption coefficient. The contribution of error can also come from the panel resonance that is more likely due to tight fitting of the sample inside the impedance tube, and due to the relatively thin sample (compared to other samples) which could generate the panel resonance. For the thicker samples, the model follows the trend of the measured absorption coefficient in a reasonably good agreement. However it should be noted that the JCA model underestimates the measured data particularly above 2.5 kHz. The disagreement on the absorption level could be due to the presence of the micro-pores in the fibers (see again Fig. 2) which can turn the DPEFB fibres into double porosity media, and this is ignored in the JCA model. The model for this type of media was proposed by Olny and Boutin [55] which takes into account the connection between the pores and the micro-pores. Thus notes must be taken on the underestimation of absorption coefficient at high frequencies when the fitted data obtained from the JCA models are to be used for predictions.

However, it is worth mentioning that unlike the optimized empirical model like the revised D&B model used in the present study, when precise values of airflow resistivity and optimization of input parameters are taken into account, the JCA model presents more accurate predictions even when applied to different types of sample materials.

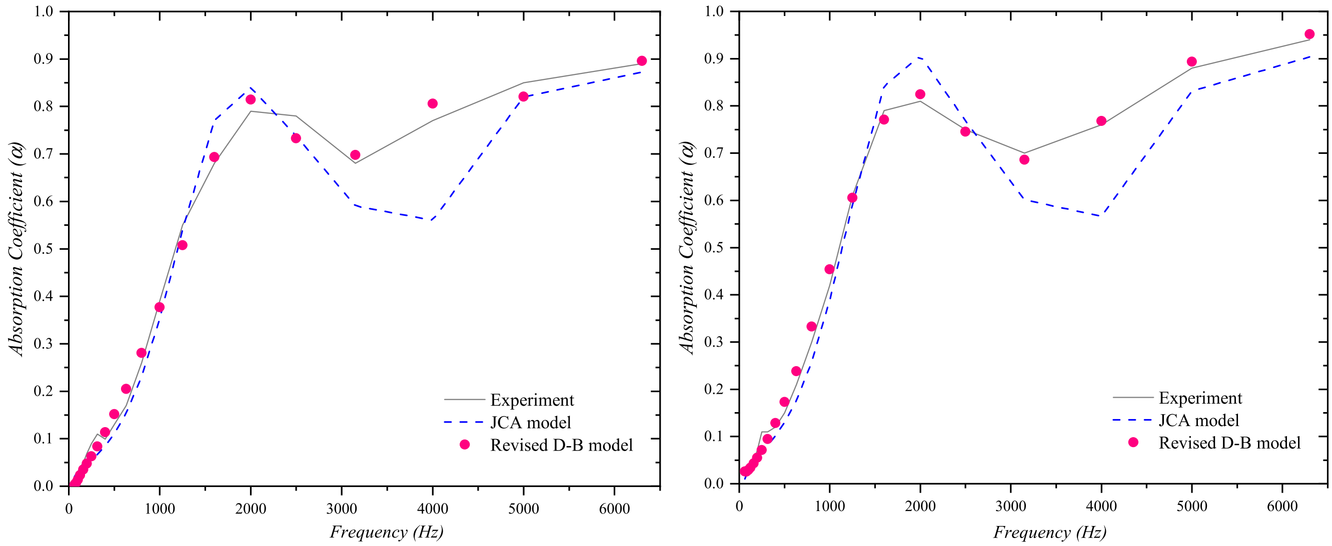

(a) Density of 100 kg/m³

(b) Density of 200 kg/m³

Fig. 10. Comparison of the sound absorption coefficients of DPEFB fibres samples (30 mm thickness) obtained from experiment vs. mathematical models.

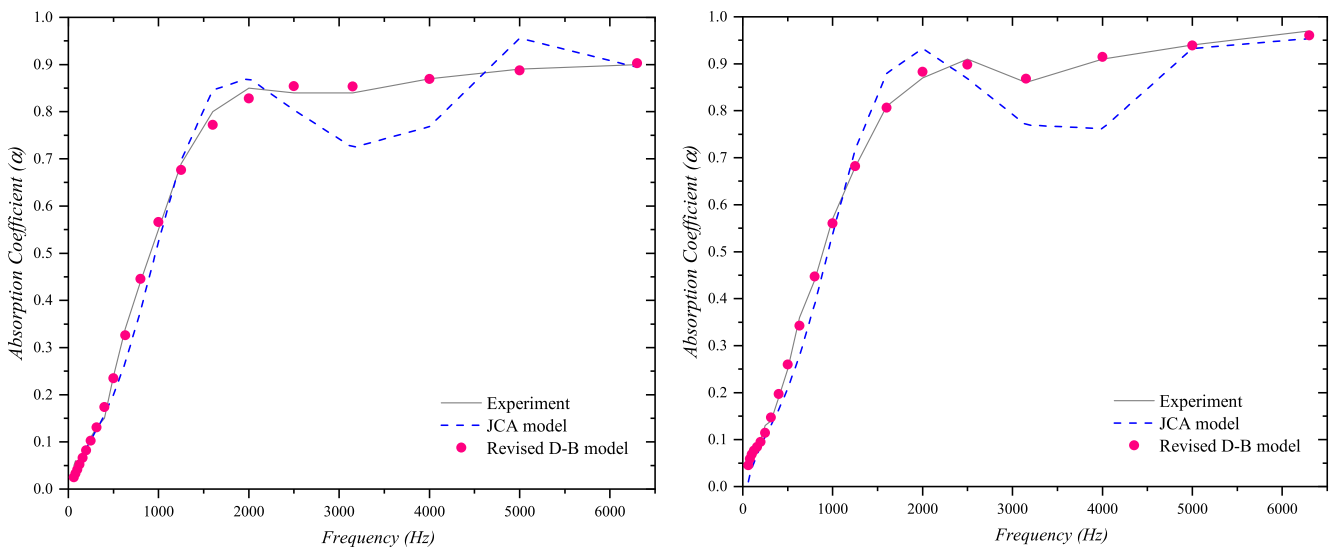

(a) Density of 100 kg/m³

(b) Density of 200 kg/m³

Fig. 11. Comparison of the sound absorption coefficients of DPEFB fibres samples (40 mm thickness) obtained from experiment vs. mathematical models.

This model has also been shown to successfully predict the sound absorption of wood-wool cement board, a material with inhomogeneous characteristic consisting of randomly distributed wood-wool strands with various dimensions [54] and the sound absorbers obtained from olive pruning wastes [3].

4. Conclusion

The use of agricultural waste from date palm empty fruit bunch (DPEFB) fibres for sound absorber has been reported. The experiment shows that for density of 100 kg/m^3 the absorption coefficient is 0.6–0.8 above 1.5 kHz for the samples with the thickness of 20 mm and 30 mm. For the thickness of 40 mm, the values even reached the value of 0.9. The values can reach 0.7–0.8 above 1 kHz for the density of 200 kg/m^3. The optimization of D&B model provides good agreement with the experimental data, while although the JCA model follows the trend of the measured absorption coefficient, it underestimates the measured data at high frequencies. The DPEFB fibers has also been shown to have comparable sound absorption performance with several other natural fibers.

Conflict of interest (COI)

The authors declare that there are no conflicts of interest.

Acknowledgements

This study is funded by Iran National Science Foundation (INSF) for the financial support of this research project [grant numbers 97014669]. Also, we are thankful to Tarbiat Modares University for providing the necessary laboratory facilities for this work.

Appendix A. Supplementary data

Supplementary data to this article can be found online at https://doi.org/10.1016/j.buildenv.2019.106274.

References

[1] K.L. Pickering, M.G.A. Efendy, T.M. Le, A review of recent developments in natural fibre composites and their mechanical performance, Compos. Appl. Sci. Manuf. 83 (2016) 98–112.
[2] L. Galbrun, L. Scerri, Sound insulation of lightweight extensive green roofs, Build. Environ. 116 (2017) 130–139.
[3] F. Martellotta, A. Cannavale, V. De Matteis, U. Ayr, Sustainable sound absorbers obtained from olive pruning wastes and chitosan binder, Appl. Acoust. 141 (2018) 71–78.
[4] E. Taban, A. Tajpoor, M. Faridan, S.E. Samaei, M.H. Beheshti, Acoustic absorption characterization and prediction of natural coir fibers, Acoust Aust. 47 (1) (2019) 67–77.
[5] X. Tang, X. Zhang, H. Zhang, X. Zhuang, X. Yan, Corn husk for noise reduction: robust acoustic absorption and reduced thickness, Appl. Acoust. 134 (2018) 60–68.
[6] A. Putra, K.H. Or, M.Z. Selamat, M.J.M. Nor, M.H. Hassan, I. Prasetiyo, Sound absorption of extracted pineapple-leaf fibres, Appl. Acoust. 136 (2018) 9–15.
[7] Z. Lim, A. Putra, M. Nor, M. Yaakob, Sound absorption performance of natural kenaf fibres, Appl. Acoust. 130 (2018) 107–114.
[8] K.H. Or, A. Putra, M.Z. Selamat, Oil palm empty fruit bunch fibres as sustainable acoustic absorber, Appl. Acoust. 119 (2017) 9–16.
[9] U. Berardi, G. Iannace, M. Di Gabriele, The acoustic characterization of broom fibers, J. Nat. Fibers 14 (6) (2017) 858–863.
[10] C. Othmani, M. Taktak, A. Zein, T. Hentati, T. Elnady, T. Fakhfakh, et al., Experimental and theoretical investigation of the acoustic performance of sugarcane wastes based material, Appl. Acoust. 109 (2016) 90–96.
[11] S. Prabhakaran, V. Krishnaraj, R. Zitoune, Sound and vibration damping properties of flax fiber reinforced composites, Procedia Engineering 97 (2014) 573–581.
[12] X. Liu, X. Yan, H. Zhang, Effects of pore structure on sound absorption of kapok-based fiber nonwoven fabrics at low frequency, Text. Res. J. 86 (7) (2016) 755–764.
[13] U. Berardi, G. Iannace, Acoustic characterization of natural fibers for sound absorption applications, Build. Environ. 94 (2015) 840–852.
[14] H. Koruk, G. Genç, Investigation of the acoustic properties of bio luffa fiber and composite materials, Mater. Lett. 157 (2015) 166–168.
[15] E. Tholkappiyan, D. Saravanan, R. Jagasthitha, T. Angeswari, V. Surya, Prediction of acoustic performance of banana fiber-reinforced recycled paper pulp composites, J. Ind. Text. 45 (6) (2016) 1350–1363.
[16] N.D. Yilmaz, N.B. Powell, P. Banks-Lee, S. Michielsen, Hemp-fiber based nonwoven composites: effects of alkalization on sound absorption performance, Fibers Polym. 13 (7) (2012) 915–922.
[17] S. Fatima, A.R. Mohanty, Acoustical and fire-retardant properties of jute composite materials, Appl. Acoust. 72 (2) (2011) 108–114.
[18] M. Hosseini Fouladi, M. Ayub, M. Jailani Mohd Nor, Analysis of coir fiber acoustical characteristics, Appl. Acoust. 72 (1) (2011) 35–42.
[19] S. Ersoy, H. Küçük, Investigation of industrial tea-leaf-fibre waste material for its sound absorption properties, Appl. Acoust. 70 (1) (2009) 215–220.
[20] T. Koizumi, N. Tsujiuchi, A. Adachi, The development of sound absorbing materials using natural bamboo fibers, WIT Trans. Built Environ. 59 (2002).
[21] A.V. Ratna Prasad, K. Mohana Rao, Mechanical properties of natural fibre reinforced polyester composites: Jowar, sisal and bamboo, Mater. Des. 32 (8) (2011) 4658–4663.
[22] S.V. Joshi, L.T. Drzal, A.K. Mohanty, S. Arora, Are natural fiber composites environmentally superior to glass fiber reinforced composites? Compos. Appl. Sci. Manuf. 35 (3) (2004) 371–376.
[23] F. Asdrubali, F. D'Alessandro, S. Schiavoni, A review of unconventional sustainable building insulation materials, Sustain. Mater. Technol. 4 (2015) 1–17.
[24] M. Jawaid, H.A. Khalil, Cellulosic/synthetic fibre reinforced polymer hybrid composites: a review, Carbohydr. Polym. 86 (1) (2011) 1–18.
[25] B.K. Tan, Y.C. Ching, S.C. Poh, L.C. Abdullah, S.N. Gan, A review of natural fiber reinforced poly (vinyl alcohol) based composites: application and opportunity, Polymers 7 (11) (2015) 2205–2222.
[26] C. Chen, Y. Zhang, G. Sun, J. Wang, G. Wang, Windmill palm fiber/polyvinyl alcohol coated nonwoven mats with sound absorption characteristics, BioResources 11 (2) (2016) 4212–4225.
[27] R. Dunne, D. Desai, R. Sadiku, A review of the factors that influence sound absorption and the available empirical models for fibrous materials, Acoust Aust. 45 (2) (2017) 453–469.
[28] C. Othmani, M. Taktak, A. Zain, T. Hantati, N. Dauchez, T. Elnady, et al., Acoustic characterization of a porous absorber based on recycled sugarcane wastes, Appl. Acoust. 120 (2017) 90–97.
[29] R. Belakroum, A. Gherfi, K. Bouchema, A. Gharbi, Y. Kerboua, M. Kadja, et al., Hygric buffer and acoustic absorption of new building insulation materials based on date palm fibers, J. Build. Eng. 12 (2017) 132–139.
[30] L.A. AL-Rahman, R.I. Raja, R.A. Rahman, Z. Ibrahim, Acoustic properties of innovative material from date palm fibre, Am. J. Appl. Sci. 9 (9) (2012) 1390.
[31] L.A. ALRahman, R.I. Raja, R.A. Rahman, Z. Ibrahim, Comparison of acoustic characteristics of date palm fibre and oil palm fibre, Res. J. Appl. Sci. Eng. Technol. 7 (8) (2014) 1656–1661.
[32] E.A. Khidir, N. Nikabdullah, M.J.M. Nor, M. Tahir, M.Z. Nuawi (Eds.), A Preliminary Study on the Sound Absorption of Self-Facing Date Palm Fibers. Applied Mechanics and Materials, Trans Tech Publ, 2014.
[33] Production-Date-2016 T. http://www.fao.org/faostat/en/#data/QC. in 17 November 2016.
[34] Maryam Gholami, Mohammad Saleh Ahmadi, M.A. Tavanaie, Mechanical properties of date palm fiber reinforced polymer composites: a review, Polymerization 7 (1) (2017) 82–93.
[35] H. Hosseinkhani, Gypsum Bounded Board Production Reinfoced with Date Palm (Phoenix Dactylifera L.) Pruning Residues Fibers, (2015).
[36] ISO 9053, Acoustics—Materials for Acoustical Applications—Determination of Airflow Resistance, (1991).
[37] R. Maderuelo-Sanz, J.M. Barrigón Morillas, M. Martín-Castizo, V. Gómez Escobar, G. Rey Gozalo, Acoustical performance of porous absorber made from recycled rubber and polyurethane resin, Lat. Am. J. Solid. Struct. 10 (3) (2013) 585–600.
[38] D.L. Johnson, J. Koplik, R. Dashen, Theory of dynamic permeability and tortuosity in fluid-saturated porous media, J. Fluid Mech. 176 (1987) 379–402.
[39] Y. Champoux, J.F. Allard, Dynamic tortuosity and bulk modulus in air-saturated porous media, J. Appl. Phys. 70 (4) (1991) 1975–1979.
[40] K.V. Horoshenkov, J.-P. Groby, O. Dazel, Asymptotic limits of some models for sound propagation in porous media and the assignment of the pore characteristic lengths, J. Acoust. Soc. Am. 139 (5) (2016) 2463–2474.
[41] M. Delany, E. Bazley, Acoustical properties of fibrous absorbent materials, Appl. Acoust. 3 (2) (1970) 105–116.
[42] M. Garai, F. Pompoli, A simple empirical model of polyester fibre materials for acoustical applications, Appl. Acoust. 66 (12) (2005) 1383–1398.
[43] Y. Miki, Acoustical properties of porous materials-Modifications of Delany-Bazley models, J. Acoust. Soc. Jpn. 11 (1) (1990) 19–24.
[44] T. Komatsu, Improvement of the Delany-Bazley and Miki models for fibrous sound-absorbing materials, Acoust Sci. Technol. 29 (2) (2008) 121–129.
[45] U. Berardi, G. Iannace, Predicting the sound absorption of natural materials: best-fit inverse laws for the acoustic impedance and the propagation constant, Appl. Acoust. 115 (2017) 131–138.
[46] J.F. Allard, Y. Champoux, New empirical equations for sound propagation in rigid frame fibrous materials, J. Acoust. Soc. Am. 91 (6) (1992) 3346–3353.
[47] Y. Atalla, R. Panneton, Inverse acoustical characterization of open cell porous media using impedance tube measurements, Can. Acoust. 33 (1) (2005) 11–24.
[48] X. Olny, R. Panneton, Acoustical determination of the parameters governing thermal dissipation in porous media, J. Acoust. Soc. Am. 123 (2) (2008) 814–824.
[49] N. Jiménez, V. Romero-García, J.-P. Groby, Perfect absorption of sound by rigidly-backed high-porous materials, Acta Acustica united Acustica 104 (3) (2018) 396–409.
[50] F.A. Everest, K.C. Pohlmann, Master Handbook of Acoustics, (2015).
[51] F.J. Fahy, Foundations of Engineering Acoustics, Elsevier, 2000.
[52] A. Santoni, P. Bonfiglio, P. Fausti, C. Marescotti, V. Mazzanti, F. Mollica, et al., Improving the sound absorption performance of sustainable thermal insulation materials: natural hemp fibres, Appl. Acoust. 150 (2019) 279–289.
[53] Z. Lim, A. Putra, M.J.M. Nor, M. Yaakob, Sound absorption performance of natural kenaf fibres, Appl. Acoust. 130 (2018) 107–114.
[54] B. Botterman, G.C.H. Doudart de la Grée, M.C.J. Hornikx, Q.L. Yu, H.J.H. Brouwers, Modelling and optimization of the sound absorption of wood-wool cement boards, Appl. Acoust. 129 (2018) 144–154.
[55] X. Olny, C. Boutin, Acoustic wave propagation in double porosity media, J. Acoust. Soc. Am. 114 (2003) 73–89.